

# Application of the Diffuse Interface Numerical Technique for Solving the Reduced Multi-component Model

[Ahmed Ballil\* and Shaban Jolgam]

**Abstract**—Numerical simulation of multi-component flows is a challenging task. It requires dealing with mathematical models, numerical solution techniques, uniformity and nonuniformity of the physical and thermodynamic properties of the flow component and the dynamic changes of the interfaces. In this contribution a numerical application is developed to solve a pressure non-equilibrium multi-component model. The numerical solution is based on a finite volume scheme and the interface is treated as a diffuse zone with a small controlled thickness. Since each flow component has its own pressure, a pressure relaxation procedure is considered during the solution. The code is verified against benchmark tests in one and two dimension flows. The results show very good agreement with the reference data, which proves the capabilities of the developed numerical tools.

**Keywords**—Compressible multi-component flows, interfaces, Godunov approach, Riemann solvers, pressure relaxation

## I. Introduction

Multi-component flows are common in many industrial applications and engineering processes. Good examples are combustion in aircraft engines, power plants, safety of chemical reactors, processes of condensation and boiling. The topic of multi-component and multi-phase flows has developed considerably during the last few decades. Recently, much research covering theoretical, experimental and computational multi-component flows have been conducted; See, for example, [1], [2], [3] and [4]. This manuscript considers computing of the evolution of interfaces in the compressible two-component flows and uses a multi-component flow algorithm to simulate these types of flows.

The main numerical methods that are commonly used for simulating compressible multi-component flows are: the Sharp Interface Methods (SIM) and the Diffuse Interface Methods (DIM).

---

Ahmed Ballil\* (*Corresponding author*)  
University of Benghazi  
Libya

Shaban Jolgam  
University of Zawia  
Libya

The Sharp interface methods are based on the elimination of the numerical diffusion at the interfaces and they could be divided into the following group of methods: Lagrangian methods [5], Arbitrary Lagrangian Eulerian methods [6], interface reconstruction methods [7], front tracking methods [8] and level set methods [9]. The main disadvantage of these methods is the complexity in the implementation, especially in three dimensional coding. Contrary to the SIM, the DIM methods allow for the numerical diffusion at the interfaces. Although the numerical diffusion is considered as a drawback of the numerical solution, it assists in tracking the discontinuity. Nevertheless, its impact on the overall solution should be controlled. There are many techniques to control the numerical diffusion zone, for example, by using high resolution schemes and grid refinement. Apart from this, the DIM has the advantage of using the similar numerical algorithm for the whole flow domain and possesses the capability to deal easily with inflow and outflow boundary conditions [10], [11] and [12].

This paper is organized as follows: section II describes the mathematical model, which is used here for the code development; the numerical method is described in section III; the verification of the code and the results obtained are presented in section IV; finally, brief conclusion is made in section V.

## II. Mathematical Model

### A. Governing Equations

The reduced two component flow model used in this work was first derived in [1] from the generic model [13]. The model was modified and developed further in [14] and [15]. The modified governing equations consist of the six partial differential equations representing a volume fraction equation, two continuity equations, the single momentum equation and the internal energy equation for each flow component. In addition to an extra equation for mixture energy which was derived from the combination of the two internal energy equations with mass and momentum equations [14]. This extra equation plays an important role during the numerical solution to circumvent the numerical difficulties related to the mechanical equilibrium of the two component model.

The system of the governing equations in one-dimensional flows without mass and heat transfer can be written in the following form:

$$\begin{aligned} \partial \alpha_1 / \partial t + u \partial \alpha_1 / \partial x &= \mu(p_1 - p_2), \\ \partial \alpha_1 \rho_1 / \partial t + \partial \alpha_1 \rho_1 u / \partial x &= 0, \\ \partial \alpha_2 \rho_2 / \partial t + \partial \alpha_2 \rho_2 u / \partial x &= 0, \\ \partial \rho u / \partial t + \partial [\rho u^2 + (\alpha_1 p_1 + \alpha_2 p_2)] / \partial x &= 0, \\ \partial \alpha_1 \rho_1 e_1 / \partial t + \partial \alpha_1 \rho_1 e_1 u / \partial x + \alpha_1 p_1 \partial u / \partial x &= -P_i \mu (p_1 - p_2), \\ \partial \alpha_2 \rho_2 e_2 / \partial t + \partial \alpha_2 \rho_2 e_2 u / \partial x + \alpha_2 p_2 \partial u / \partial x &= P_i \mu (p_1 - p_2). \end{aligned} \quad (1)$$

The extra mixture energy equation is:

$$\partial (\rho E) / \partial t + \partial u [\rho E + (\alpha_1 p_1 + \alpha_2 p_2)] / \partial x = 0. \quad (2)$$

Where  $\alpha_k$  is the volume fraction of the component  $k$ .  $\rho_k, p_k$  and  $e_k$  are respectively the density, pressure and internal energy of the  $k^{\text{th}}$  component of the flow.  $\mu$  is a positive homogenization parameter controlling the rate at which the pressure tends to the equilibrium state.  $P_i$  is the pressure at the interface.  $u$  is the mixture velocity,  $\rho$  is the mixture density and  $E$  is the total mixture energy.

### B. Closure Relations

It is clear that the number of unknown variables is larger than the number of equations. Therefore, the following relations are necessary to close the model:

- The saturation condition of volume fraction:

$$\alpha_1 + \alpha_2 = 1 \quad (3)$$

- The relations of the mixture variables:

Mixture density:

$$\rho = \alpha_1 \rho_1 + \alpha_2 \rho_2 \quad (4)$$

Mixture velocity:

$$u = (\alpha_1 \rho_1 u_1 + \alpha_2 \rho_2 u_2) / \rho \quad (5)$$

Mixture pressure:

$$p = \alpha_1 p_1 + \alpha_2 p_2 \quad (6)$$

Mixture internal energy:

$$e = (\alpha_1 \rho_1 e_1 + \alpha_2 \rho_2 e_2) / \rho \quad (7)$$

Mixture total energy:

$$E = e + u^2/2 \quad (8)$$

- The formula of the interfacial pressure:

$$P_i = (z_2 p_1 + z_1 p_2) / (z_1 + z_2) \quad (9)$$

Where  $z_k = \rho_k c_k$  is the acoustic impedance of the component  $k$  of the flow and  $c$  refers to the speed of sound.

- The equation of state (EOS) for each fluid. In this work the stiffened EOS is considered for gases and liquids:

$$p_k = (\gamma - 1) \rho_k e_k - \gamma_k \pi_k \quad (10)$$

where  $\gamma$  is the heat capacity ratio and  $\pi$  is a pressure constant, which depends on the working fluids.

## III. Numerical Method

The numerical method, which is considered for solving the two-component governing equations, takes into account the discretization of the non-conservative equations and non-conservative terms that exist in the model (1). The numerical technique is developed based on the principle of the Strang splitting method [16], where the solution of the model is divided into two parts. The first part is the hyperbolic operator and the second part is the pressure relaxation operator, which are solved in succession at each time step.

### A. Hyperbolic Operator

The hyperbolic operator of the governing equations can be rewritten in the following compact form:

$$\begin{aligned} \partial \alpha_1 / \partial t + u \partial \alpha_1 / \partial x &= 0, \\ \partial U / \partial t + \partial F(U) / \partial x &= 0. \end{aligned} \quad (11)$$

where the conservative vector  $U$  is given as  $U = (\alpha_1 \rho_1, \alpha_2 \rho_2, \rho u, \rho E)^T$  and the flux vector is given as  $F(U) = (\alpha_1 \rho_1 u, \alpha_2 \rho_2 u, \rho u^2 + p, u(\rho E + p))^T$ .

The hyperbolic operator is solved using an extended finite volume Godunov approach. The classical Monotonic Upstream-centered Scheme for Conservation Laws (MUSCL) scheme is utilized to achieve second order accuracy in terms of the primitive variables [17].

The explicit Godunov scheme can be written as follows:

$$U_i^{n+1} = U_i^n - \Delta t / \Delta x [F(U^*(U_i, U_{i+1})) - F(U^*(U_i, U_{i-1}))] \quad (12)$$

Equation (12) is applied to the mass, momentum and total energy equations, where the flux functions are obtained using the extended VFRoe and HLLC approximate Riemann solvers for Euler equations [17].

Similarly, the non-conservative equations for the volume fraction and two internal energies are discretized as follows:

$$\begin{aligned} \alpha_i^{n+1} &= \alpha_i^n - \Delta t / \Delta x u_i [(u \alpha_i)^*_{i+1/2} - (u \alpha_i)^*_{i-1/2} \\ &\quad - \alpha^n_{1i} (u^*_{i+1/2} - u^*_{i-1/2})] \end{aligned} \quad (13)$$

$$\begin{aligned} (ape)_{ki}^{n+1} &= (ape)_{ki}^n - \Delta t / \Delta x u_i [(apeu)^*_{ki+1/2} - (apeu)^*_{ki-1/2} \\ &\quad - (ap)^n_{ki} (u^*_{i+1/2} - u^*_{i-1/2})] \end{aligned} \quad (14)$$

### B. Pressure Relaxation Operator

After the solution of the hyperbolic operator is accomplished, in each time step a relaxation solver is applied to modify the pressure field. For the pressure relaxation operator, the system (15) is solved based on the instantaneous pressure relaxation assumption, where the variable  $\mu$  in the relaxation terms is considered to be infinite. The procedure 4 of the iterative relaxation method introduced in [18] is utilized to perform the direct integration of the system (15).

$$\begin{aligned}
 \partial \alpha_1 / \partial t &= \mu(p_1 - p_2), \\
 \partial \alpha_1 \rho_1 / \partial t &= 0, \\
 \partial \alpha_2 \rho_2 / \partial t &= 0, \\
 \partial \rho u / \partial t &= 0, \\
 \partial \alpha_1 \rho_1 e_1 / \partial t &= -P_i \mu(p_1 - p_2), \\
 \partial \alpha_2 \rho_2 e_2 / \partial t &= P_i \mu(p_1 - p_2), \\
 \partial (\rho E) / \partial t &= 0.
 \end{aligned} \tag{15}$$

The computed volume fraction and the mixture energy  $\rho e$  are used to obtain the mixture pressure from the mixture equation of state (16).

$$P = [\rho e - \sum(\alpha_k \gamma_k \pi_k / \gamma_k - 1)] / \sum(\alpha_k / \gamma_k - 1) \tag{16}$$

## IV. Numerical Tests and Results

Two benchmark numerical experiments are considered to verify the reliability and the accuracy of the developed numerical algorithm. The first case study is the classical one-dimensional water-air shock tube test and the second is the two-dimensional interface translation test.

### A. Water-Air Shock Tube

The water-air shock tube test is widely used for assessing numerical algorithms; see for instance [3] and [11]. This case enables the verification of the implemented numerical tools using the idealized analytical solution. The length of the tube (computational domain) is 1 m with the initial diaphragm located at  $x_0 = 0.7$  m. The initial conditions of water and air are summarized in table I. The water on the left side of the diaphragm has a higher pressure than the air on the right side. Due to the high pressure ratio ( $10^4$ ), as soon as the diaphragm is removed a strong shock and contact waves propagate to the right and a rarefaction wave propagates to the left. In order to start the computation, the volume of the air in the water side is considered to be only  $10^{-8}$  and vice versa in the air side. The computations are conducted using the VFRoe Riemann solver with 100 and 1000 computational cells and a Courant-Friedrichs-Lewy number (CFL) of 0.6. The results for the gas volume fraction, velocity, pressure and the mixture density are shown in Figs. 1 to 4 at time  $229 \mu s$ . A very good agreement between the numerical and exact solutions can be seen especially with the grid resolution of 1000 cells.

TABLE I. INITIAL CONDITIONS OF WATER-AIR SHOCK TUBE

| Physical properties           | $x_0 \leq 0.7$ |        | $x_0 > 0.7$    |        |
|-------------------------------|----------------|--------|----------------|--------|
|                               | Water          | Air    | Water          | Air    |
| Density (kg/m <sup>3</sup> )  | 1000           | 50     | 1000           | 50     |
| Pressure (Pa)                 | $10^9$         | $10^9$ | $10^5$         | $10^5$ |
| Velocity (m/s)                | 0.0            | 0.0    | 0.0            | 0.0    |
| Heat capacity ratio, $\gamma$ | 4.4            | 1.4    | 4.4            | 1.4    |
| Pressure constant, $\pi$      | $6 \cdot 10^8$ | 0.0    | $6 \cdot 10^8$ | 0.0    |

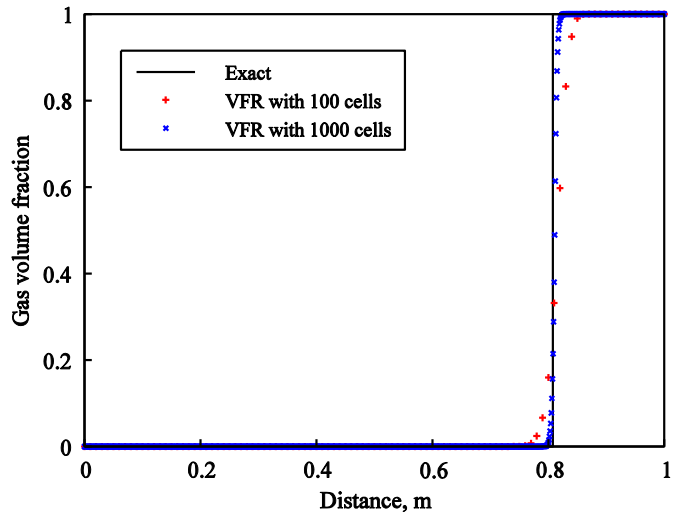


Figure 1. Gas volume fraction for water-air shock tube at time  $t = 229 \mu s$ .

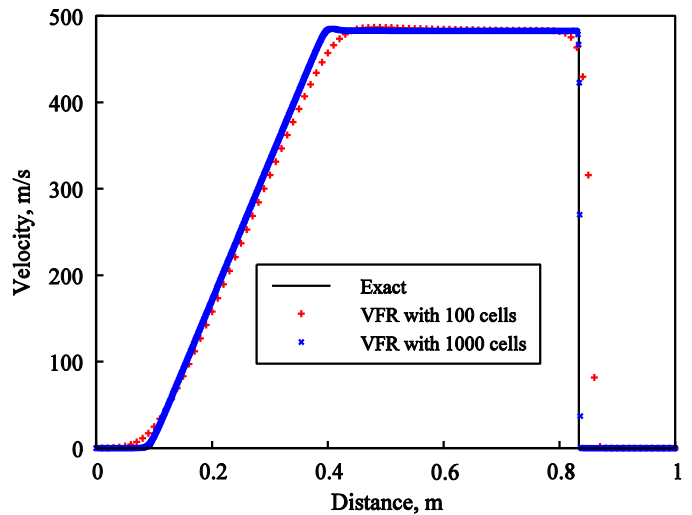


Figure 2. Velocity profile for water-air shock tube at time  $t = 229 \mu s$ .

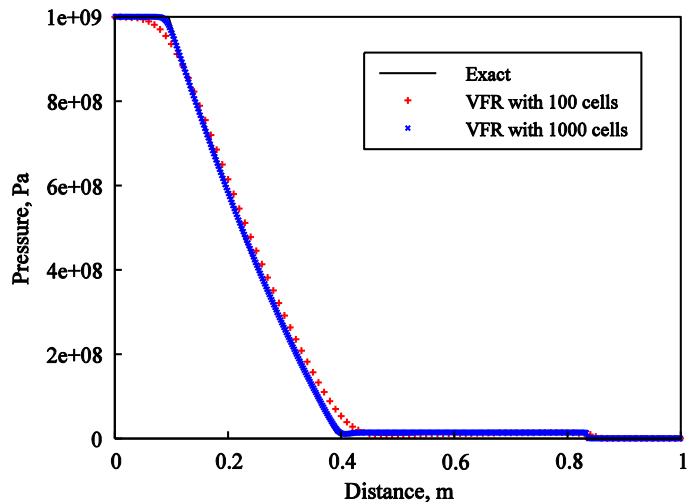


Figure 3. Pressure profile for water-air shock tube at time  $t = 229 \mu s$ .

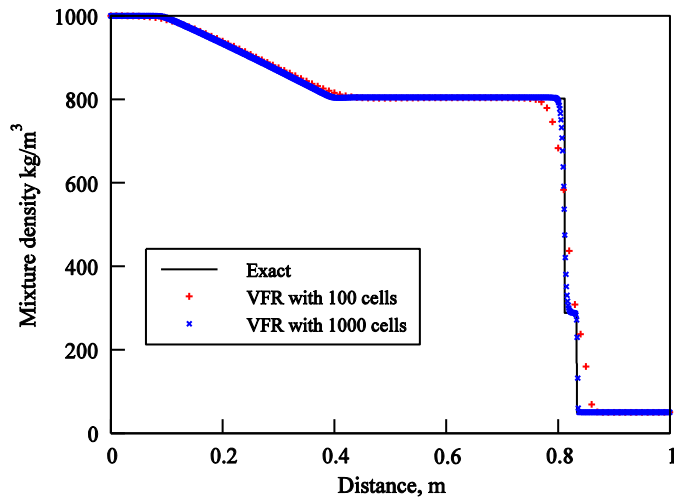


Figure 4. Pressure profile for water-air shock tube at time  $t = 229 \mu s$ .

### B. Interface Translation Test

This is a classical two-dimensional test which is widely used for testing the numerical codes; see for example [10]. It allows observing any velocity or pressure oscillations at the interfaces. The physical domain consists of a square of  $1 \times 1 \text{ m}^2$  contains a circular interface moving with uniform velocity and pressure in a gas/gas medium. The initial conditions for the working fluids are presented in table II. A schematic diagram of the computational domain associated with the boundary conditions are illustrated in Fig. 5. The computation is carried out using the HLLC Riemann solver with a high grid resolution of  $700 \times 700$  computational cells and a  $CFL = 0.3$ .

TABLE II. INITIAL CONDITIONS OF THE INTERFACE TRANSLATION TEST

| Physical properties           | Circular interface | Surrounding gas |
|-------------------------------|--------------------|-----------------|
| Density ( $\text{kg/m}^3$ )   | 1.0                | 0.1             |
| Pressure (Pa)                 | 1.0                | 1.0             |
| X-component of velocity (m/s) | 1.0                | 1.0             |
| Y-component of velocity (m/s) | 1.0                | 1.0             |
| Heat capacity ratio, $\gamma$ | 1.4                | 1.6             |

The result of volume fraction contour at time  $t = 0.36 \text{ s}$  is shown in Fig. 6, where the circular interface translated from the initial position at  $x = 0.25 \text{ m}$  and  $y = 0.25 \text{ m}$  to the new position of  $x = 0.61 \text{ m}$  and  $y = 0.61 \text{ m}$ . The pressure distribution in the domain is presented in Fig. 7, where the uniformity in pressure with no pressure oscillations across the interfaces can be observed. The results show very good agreement with other results; see for example [10] and [19].

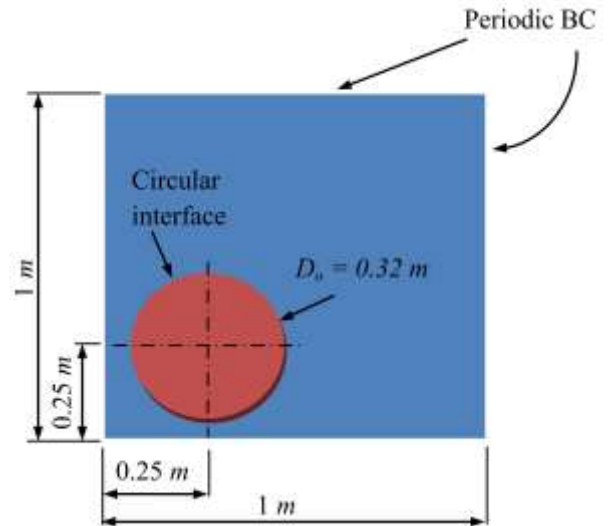


Figure 5. Schematic diagram with initial and boundary conditions of the interface translation test.

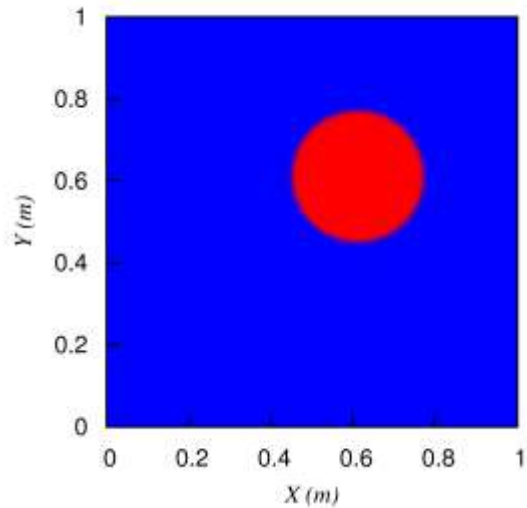


Figure 6. Volume fraction contour at time  $t = 0.36 \text{ s}$ .

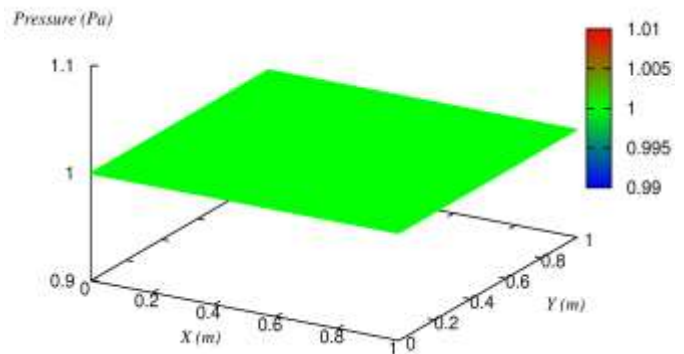


Figure 7. Pressure distribution at time  $t = 0.36 \text{ s}$ .

## v. Conclusion

In this paper a numerical algorithm was developed to solve the reduced multi-component model. The code was verified using benchmark numerical tests. The numerical results show very good agreement with the reference data. The diffusivity of the numerical technique was restricted and controlled using high order scheme and high grid resolution. The developed numerical tools can be utilized for further investigations in the field of multiphase and multi-component flows.

## References

- [1] A. K. Kapila, R. Menikoff, J. B. Dzil, S. F. Son, and D. S. Stewart, "Two-phase modeling of deflagration to detonation transition in granular materials: Reduced equations," *Physics of Fluids*, vol. 13, pp. 3002 – 3024, 2001.
- [2] G. Layes, G. Jourdan, and L. Houas, "Experimental study on a plane shock wave accelerating a gas bubble," *Physics of Fluids*, vol. 21, 074102, 2009.
- [3] R. Saurel, and R. Abgrall, "A multiphase Godunov method for compressible multifluid and multiphase flows," *Journal of Computational Physics*, vol. 150, pp. 425 – 467, 1999.
- [4] A. Ballil, S. A. Jolgam, A. F. Nowakowski, and F. C. G. A. Nicolleau, "Computing Compressible Two-Component Flow Systems Using Diffuse Interface Method," In *IAENG Transactions on Engineering Technologies*, Vol. 229 of *Lecture Notes in Electrical Engineering*, Gi-Chul Yang, Sio-long Ao and Len Gelman, Eds. Springer Netherlands, 2013, pp. 135 – 146.
- [5] D. J. Benson, "Computational methods in Lagrangian and Eulerian hydrocodes," *Computer Methods in Applied Mechanics and Engineering*, vol. 99, pp. 235 – 394, 1992.
- [6] C. Farhat, and F. X. Roux, "A method of finite element tearing and interconnecting and its parallel solution algorithm," *International Journal for Numerical Methods in Engineering*, vol. 32, pp. 1205 – 1227, 1991.
- [7] D.L. Youngs, *Time-dependent multi-material flow with large fluid distortion*. Academic Press, 1982.
- [8] R. J. LeVeque, and K. M. Shyue, "Two-dimensional front tracking based on high resolution wave propagation methods," *Journal of Computational Physics*, vol. 123, pp. 354 – 368, 1996.
- [9] R. Fedkiw, T. Aslam, B. Merriman, and S. Osher, "A non-oscillatory Eulerian approach to interfaces in multimaterial flows (the Ghost Fluid Method)," *Journal of Computational Physics*, vol. 152, pp. 457 – 492, 1999.
- [10] K. M. Shyue, "An Efficient Shock-Capturing Algorithm for Compressible Multicomponent problems," *Journal of Computational Physics*, vol. 142, pp. 208 – 242, 1998.
- [11] R. Saurel, and O. Le Métayer, "A multiphase model for compressible flows with interfaces, shocks detonation waves and cavitation," *Journal of Fluid Mechanics*, vol. 431, pp. 239 – 271, 2001.
- [12] A. Murrone, and H. Guillard, "A five-equation reduced model for compressible two phase flow problems," *Journal of Computational Physics*, vol. 202, pp. 664 – 698, 2005.
- [13] M. R. Baer, and J. W. Nunziato, "A two-phase mixture theory for the deflagration-to-detonation transition (DDT) in reactive granular materials," *International Journal of Multiphase Flow*, vol. 12, pp. 861 – 889, 1986.
- [14] R. Saurel, F. Petitpas, and R. A. Berry, "Simple and efficient relaxation methods for interfaces separating compressible fluids, cavitating flows and shocks in multiphase mixtures," *Journal of Computational Physics*, vol. 228, pp. 1678 – 1712, 2009.
- [15] A. Zein, M. Hantke, and G. Warnecke, "Modeling phase transition for compressible two-phase flows applied to metastable liquids," *Journal of Computational Physics*, vol. 229, pp. 2964 – 2998, 2010.
- [16] G. Strang, "On the construction and comparison of difference schemes," *SIAM J. Numer. Anal.*, vol. 5, pp. 506 – 517, 1968.
- [17] E. Toro, *Riemann Solvers and Numerical Methods for Fluid Dynamics*, Springer, 1999.
- [18] M. H. Lallemand, and R. Saurel, "Pressure relaxation procedures for multiphase compressible flows," *INRIA Research Report*, No. 4038, 2000.
- [19] H. W. Zheng, C. Shu, and Y. T. Chew, and N. Qin, "A solution adaptive simulation of compressible multi-fluid flows with general equation of state," *International Journal for Numerical Methods in Fluids*, vol. 67, pp.616 – 637, 2011.